Photoelectron spectroscopic study of Sr_xNbO_3

Kazuyuki Isawa, Rittaporn Itti, Jun Sugiyama, Naoki Koshizuka, and H. Yamauchi
Superconductivity Research Laboratory, International Superconductivity Technology Center, 10-13 Shinonome 1-chome, Koto-ku, Tokyo 135, Japan
(Received 16 August 1993)

X-ray and ultraviolet photoelectron spectroscopic (XPS and UPS) data were obtained for Sr_xNbO_3 ($x=0.8,0.85,0.9$). The valency of the Nb ion was found to be between pentavalent and tetravalent. No shifts of the XPS core-level spectra, such as O 1*s*, Sr 3*p*, and Sr 3*d*, were observed in this system even when x was varied. For all samples, sharp Fermi edges were observed with He I (21.2 eV) photon excitation. The results indicate that this valence band was mainly caused by the hybridization between the O 2*p* and Nb 4*d* orbitals, as had been proposed for the tungsten bronze by Goodenough. Eu substituted samples, $(Sr,Eu)_{0.9}NbO_3$, were also studied. An additional sharp peak, due to Eu 4*f* state, was clearly observed in the valence-band region close to the Fermi level.

I. INTRODUCTION

Since the discovery of high-temperature superconductors (HTSC), transition-metal oxides with the ABO_3-type perovskite structure have been extensively studied[1-8] because the structures of HTSC cuprates are closely related to that of perovskite. Comparing the $(3d)^9$ configuration of the copper ion in the HTSC copper oxides, cations with a single electron in their *d* state, such as V^{4+} $(3d)^1$ and Nb^{4+} $(4d)^1$, both having a $S=\frac{1}{2}$ state, are of particular interest. Among the Nb oxides, Sr_xNbO_3 ($x<1$) are known to have the cubic perovskite structure[9,10] in which the Nb ions exhibit a $(4d)^1$ configuration with $S=\frac{1}{2}$.[11]

Recently, we successfully synthesized[12] polycrystalline single-phase samples of Sr_xNbO_3 with different values of x, in the range of $0.75<x\leq 0.90$, and studied[12,13] the transport properties of Sr_xNbO_3 including the temperature (T) dependence of electrical resistivity (ρ), magnetic susceptibility (χ), thermoelectric power (S), and Hall coefficient (R_H) below 300 K. We concluded that Sr_xNbO_3 ($x=0.80$, 0.85, and 0.90) should be considered to be conventional metallic conductors for two reasons. (i) The magnitude of ρ was the order of $\sim 1\times 10^{-3}$ Ω cm and ρ decreased with decreasing temperature. (ii) Assuming a single-band model, the carrier density (n) was estimated to be $n\sim 10^{22}$ cm^{-3} from the R_H measurement. However, there are several features that Sr_xNbO_3 are different from simple metals in terms of transport properties: (a) The relationship between S and T was nonlinear. (b) The R_H was weakly dependent on temperature. (c) The metallic parameter $k_F l_{tr}$ (in which k_F is the Fermi wave number and l_{tr} is the transport mean free path) was rather small being approximately unity. (This value for typical metals is $k_F l_{tr}\gg 1$.) (d) The increase in magnetoresistance ($\Delta\rho/\rho$) at $H=6$ T was estimated to be 1.5–3 % in 1.5 K.

From the above experimental data, we pointed out[12,13] that the transport properties of Sr_xNbO_3 ($0.75<x\leq 0.90$) were considered to be similar to those of amorphous metals rather than those of conventional metallic conductors. Such "amorphousness" was thought to be caused by random distribution of vacancies in the Sr sites, which deteriorated the periodicity of the lattice potential. On the other hand, we have already reported[14] the synthesis of single-phase Eu-doped $Sr_{0.9}NbO_3$ samples, $Sr_{0.9-y}Eu_yNbO_3$ for $0\leq y\leq 0.9$, and this system was metallic at all ranges of y. It is worth elucidating whether the electronic structure was changed by Eu doping.

Photoelectron spectroscopic analysis of the core levels and that of the valence band can provide information on the nature of bonding such as valence and that on the electronic structure, respectively. However, to our knowledge, such data are not yet available for Sr_xNbO_3.

In this paper, photoelectron measurements were performed to investigate the electronic structure of Sr_xNbO_3 for different values of x, and the results are reported here. Furthermore, we compared the electronic structure, especially density of states in the vicinity of E_F between Sr_xNbO_3 and $Sr_{0.9-y}Eu_yNbO_3$.

II. EXPERIMENTAL

Polycrystalline samples of Sr_xNbO_3 and $Sr_{0.9-y}Eu_yNbO_3$ were prepared by a solid-state reaction technique using reagent-grade SrO Eu_2O_3 and Nb_2O_5 powders. Stoichiometric mixtures were pressed into rectangular bars of $2\times 2\times 20$ mm^3. Each bar was encapsulated in an evacuated silica tube. In order to prepare samples in reducing atmospheres, TiO powder was used as the reducing agent. Encapsulated samples were fired at 1050 °C for 80–160 h. Powder x-ray-diffraction studies and electron probe microanalysis indicated that both Sr_xNbO_3 ($x=0.80$, 0.85, and 0.90) and $Sr_{0.9-y}Eu_yNbO_3$ ($0\leq y\leq 0.9$) samples were single phase of cubic perovskite structures. The oxygen content of the samples was determined by thermogravimetric measurements and by an inert gas fusion nondispersive IR method. As previously reported,[12,15] the oxygen deficiency (δ), for all samples was nearly zero ($\delta=0$). Thus, in the Sr_xNbO_3 samples with $x=0.80$, 0.85, and 0.90, the average Nb valen-

cies are expected to be 4.4, 4.3, and 4.2, respectively. The characterization and physical properties of the samples are reported in detail elsewhere.[12–15]

The photoelectron spectroscopic measurements were carried out in an ultrahigh-vacuum system equipped with an Al x-ray source (1486.6 eV) for x-ray photoelectron spectroscopy (XPS) and a noble-gas discharge lamp for ultraviolet photoelectron spectroscopy (UPS). The energy distribution of the photoelectron was determined by an electron energy analyzer, the resolution of which was set at 0.7 and 0.15 eV for XPS and UPS measurements, respectively. Core-level binding energies were referenced to the adventitious C 1*s* peak at 285.0 eV. For the UPS measurement, the Fermi energy was determined directly from the zero binding energy of the analyzer, because no charge up was observed and the accuracy was better than 0.15 eV. The typical pressure during the measurements was $\sim 2\times 10^{-10}$ torr. The sample was scraped in vacuum by a diamond file prior to each measurement. In this study, all of the spectra were taken at ambient temperature.

III. RESULTS AND DISCUSSION

The O 1*s* core-level XPS spectra from Sr_xNbO_3 ($x = 0.80$, 0.85, and 0.90) are shown in Fig. 1(a). The O 1*s* XPS spectrum can be usually used to check the quality of a sample and its surface under measurement.[7] For the

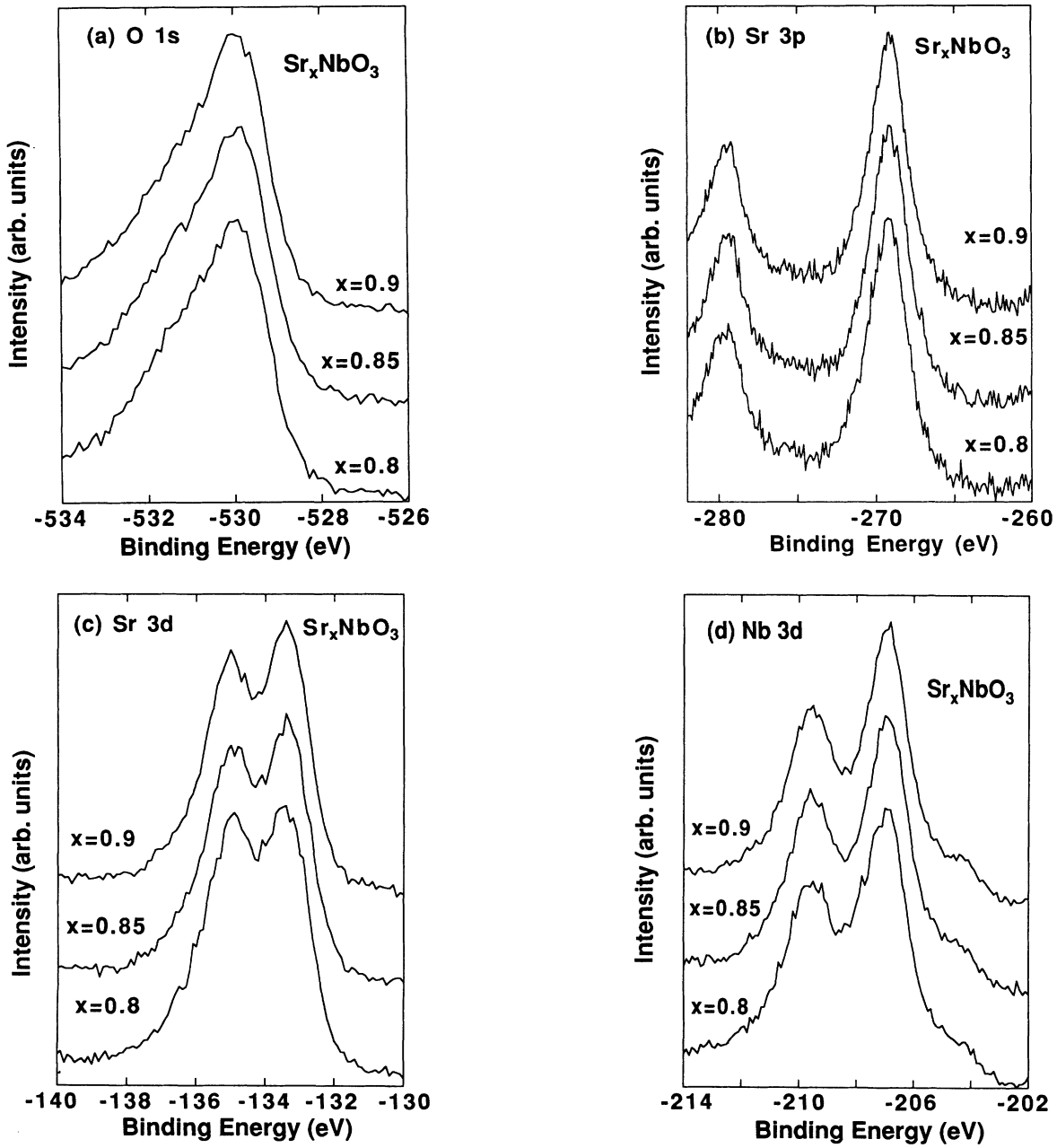

FIG. 1. XPS spectra of (a) O 1*s*, (b) Sr 3*p*, (c) Sr 3*d*, and (d) Nb 3*d* from Sr_xNbO_3 ($x = 0.8$, 0.85, 0.9) samples.

O 1s level in Sr_xNbO_3, only an intrinsic peak around 529 eV was observed for all the samples. This assures the high quality of the samples. Figures 1(b) and 1(c) show the Sr 3p and Sr 3d core-level XPS spectra from the samples, respectively. From the Sr 3p core-level spectrum, two sharp peaks were observed around 279 eV and 269 eV, which are, respectively, Sr $3p_{1/2}$ and Sr $3p_{3/2}$. The Sr $3d_{3/2}$ and Sr $3d_{5/2}$ peaks appeared around 134 eV binding energy are shown in Fig. 1(c). The Nb 3d core-level spectra are shown in Fig. 1(d). The Nb $3d_{5/2}$ peak and Nb $3d_{3/2}$ peak were, respectively, observed at 207.0 and at 209.5 eV. Since, the binding energies of the Nb $3d_{5/2}$ spectrum from NbO_2 (Nb^{4+}) and Nb_2O_5 (Nb^{5+}) are, respectively, observed at 205 and 207.5 eV,[16] the present results show that the valency of Nb^{+p} ions in the present Sr_xNbO_3 samples is between 4+ and 5+. This is consistent with our previous data, i.e, $4.2 \leq p \leq 4.4$, because the oxygen deficiency for every sample was negligible.[12,15] Though it is interesting to know how the Nb valence would change upon varying the Sr content x, it was not clearly seen in the present study, since, the changes in the binding energy of Nb with respect to x was very small. It is worth to note that, as is shown in Figs. 1(a)–1(c), the O 1s, Sr 3p, and Sr 3d core-level XPS spectra showed no significant changes in binding energies with increasing x from 0.80 to 0.90.

Figure 2(a) shows the valence-band spectra for $Sr_{0.8}NbO_3$ measured by XPS ($h\nu = 1486.6$ eV) and UPS (He I = 21.2 eV, He II = 40.8 eV). One notices that the consistency among these observed XPS and UPS peaks is fairly good. Each spectra consists of a broad peak at ~ 6 eV which primarily consists of O 2p states similar with the isostructural compounds such as $SrVO_3$.[3,4] The higher-energy resolution of UPS techniques give a spectrum with more detailed structures. At the vicinity of the Fermi level, it seems that the spectrum is enhanced and sharp Fermi edge was observed only in the case of He I UPS but not for He II or XPS cases. This is clearly shown in the bottom spectrum of Fig. 2(a). These features are common to all samples with different x's. The lack of state around E_F for He II UPS and XPS excitation are likely to be due to the difference of photoemission cross section from the Sr_xNbO_3 samples which depend on the photon energies. Since, it is widely known that the O 2p cross section shows resonance around He I photon energy, and gradually decreases with increasing photon energy,[4,17,18] the results seem to indicate that O 2p states involve strongly in the electronic states close to the Fermi level. In order to understand the detailed electronic structure at E_F, the He I UPS spectra in the vicinity of E_F are shown in Fig. 2(b) for the Sr_xNbO_3 samples with $x = 0.80$, 0.85, and 0.90. For each sample, a sharp edge and finite density of states can be clearly observed at the E_F. In general, the observation of a sharp Fermi edge is rather difficult for metallic oxides due to the surface oxygen deterioration. However, we successfully observed a sharp Fermi edge in the present case for Sr_xNbO_3 sample. This strongly suggests that the density of state at the E_F is high. And from the peak feature of this sharp edge it seems that there exists a narrow or rather flat band crossing the E_F in this metallic Sr_xNbO_3 system. The observation of the Fermi edge is consistent with previous transport data[11,12] showing metallic resistivity behavior for Sr_xNbO_3 at 300 K ($\rho \sim 1 \times 10^{-3}$ Ω cm). To our knowledge, there is no band-structure calculation for Sr_xNbO_3 available. However, the results shown in Figs. 2(a) and 2(b) indicated that the conduction band of Sr_xNbO_3 basically arises from the hybridization between the Nb 4d and O 2p orbitals, being similar to the case of tungsten-bronze compounds[19] or ReO_3.[20] This will be discussed in detail later.

Previously, we reported that carrier concentration was increased with increasing x by Hall measurements[13] and thermoelectric power.[12] Nevertheless, we could not observe drastic change in the valence-band spectra for the sample with $x = 0.80$, 0.85, and 0.90. This is probably because, for every sample, the carrier density (n) was es-

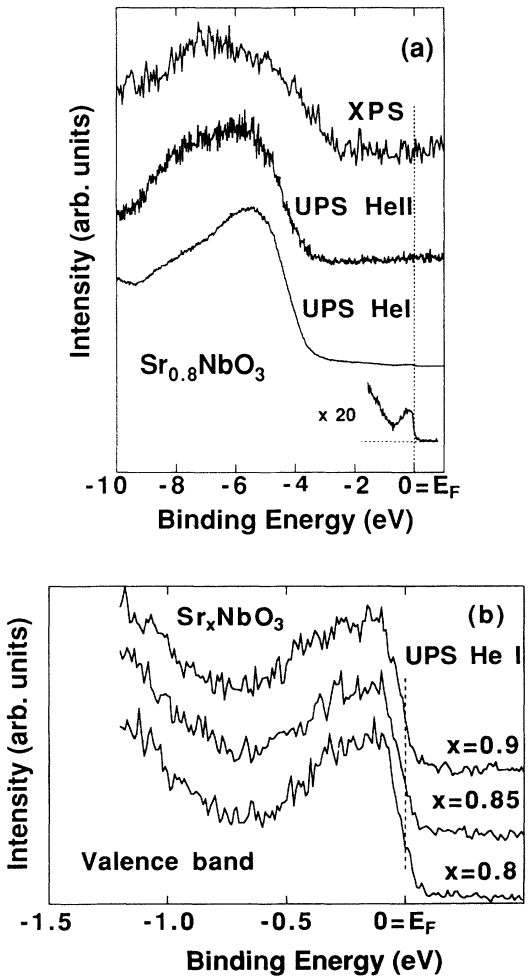

FIG. 2. (a) Comparison of valence-band spectra obtained by XPS ($h\nu = 1486.6$ eV), He II UPS ($h\nu = 40.8$ eV) and He I UPS ($h\nu = 21.2$ eV) from $Sr_{0.8}NbO_3$ sample. The Fermi edge is clearly observed only in the He I UPS spectrum. The enhancement of the He I UPS spectra in the Fermi-level region is also shown. (b) Valence-band He I UPS spectra in the vicinity of E_F from Sr_xNbO_3 ($x = 0.8$, 0.85, 0.9) samples. A clear sharp Fermi edge was observed for all samples.

timated to be same order, i.e., $\sim 10^{-22}$ cm^{-3}.[13] On the other hand, we pointed out that[12] the band-structure might change around $x = 0.90$, because the magnetic susceptibility χ was Pauli paramagnetic for the sample with $x = 0.80$ and 0.85, though χ for the $Sr_{0.9}NbO_3$ sample exhibited Curie-Wiess behavior. Since the characteristic electronic structure was approximately the same for every sample, this Curie-Wiess behavior may be attributed to other reasons such as (i) inequivalent sites for Nb ions[21] and/or (ii) stacking faults,[22] which we pointed out in Ref. 12.

Recently, Fujimori *et al.*[3] reported the photoemission spectrum in the *d*-band region of a series of Mott-Hubbard-type oxides with d^1 electronic configuration, namely, $YTiO_3$, $LaTiO_3$, $SrVO_3$, VO_2, ReO_3. Especially, the following properties were observed for $SrVO_3$ and ReO_3: (i) In $SrVO_3$, the *d* band consists of two structures; one is within ~ 1 eV of E_F with a sharp Fermi cutoff, which was assigned to itinerant *d*-band states, and the other is a broad feature centered ~ 1.5 eV below E_F, which was assigned to a remnant of the lower Hubbard band. In addition, they pointed out[3] the apparent discrepancy between this photoemission spectrum and band-structure calculation. (ii) In ReO_3, a sharp peak near E_F was observed at ~ 1 eV, and no trace was found within ~ 1 eV. Note that this photoemission spectrum were in reasonable agreement with band-structure calculations.[20]

Since the Nb^{4+} ions of Sr_xNbO_3 are known to have a $(4d)^1$ configuration,[11] it is worthwhile to discuss the conduction band in the *d* state of the structurally related compounds such as $SrVO_3$ $\{V^{4+}\ (3d)^1\}$ (Ref. 23) and ReO_3 $\{Re^{6+}\ (5d)^1\}$ (Ref. 22). It is known that[19] the covalent mixing with ions is larger for 5*d* orbitals than for 4*d* orbitals, and for 4*d* than for 3*d* orbitals. Thus, we may roughly predict that the band structure for Sr_xNbO_3 is moderate between $SrVO_3$ and ReO_3 except for a slight difference in the energy position. As seen in Fig. 2(b), for every sample, the detail structure of the valence band for Sr_xNbO_3 at ~ 1 eV was rather similar to $SrVO_3$ as reported in Ref. 3, especially a trace clearly observed within ~ 1 eV. This may indicate that the electronic structure of Sr_xNbO_3 is closer to $SrVO_3$ rather than ReO_3, even if the vacancy of Sr ions are located randomly on the *A* site in the regular perovskite structure. Indeed, the *T* vs ρ curve for $SrVO_3$ showed[2,23] rather similar behavior with Sr_xNbO_3, that is, the ρ at 300 K was $\sim 1 \times 10^{-3}$ Ω cm and ρ decreased gradually with decreasing temperature.

Figure 3 shows the XPS spectrum of the valence-band region for the $Sr_{0.9-y}Eu_yNbO_3$ ($y = 0$, 0.3, 0.5, and 0.9) samples. The following marked difference was observed between the bottom spectrum and three other spectra: For the samples with Eu (≥ 0.3), a sharp peak was observed very close to E_F. This relative enhancement of the peak at ~ 1 eV is considered to be of the Eu 4*f* characteristics. Though the valency of doped Eu ion in these materials was found to be in between 3+ ($|4f^6\rangle$) and 2+ ($|4f^7\rangle$) by XPS analysis for Eu 3*d* core-level spectra,[14] it is not clear to what extent these 4*f* states contribute to the conductivity of the samples. Note that, every sample exhibited rather similar temperature dependence of ρ, i.e., the magnitude of ρ at 300 K is the order of 1×10^{-3} Ω cm and ρ decreased monotonically with decreasing temperature.[14,24]

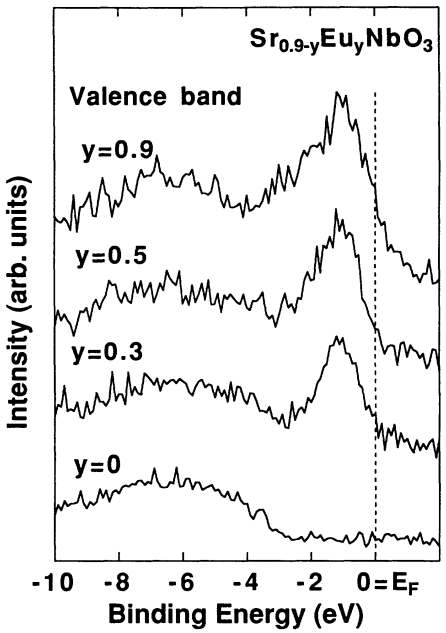

FIG. 3. Valence-band XPS spectra from $Sr_{0.9-y}Eu_yNbO_3$ with $y = 0$, 0.3, 0.5, 0.9 samples. The peak in the vicinity of the E_F due to Eu 4*f* states increased with increasing *y*.

The schematic electronic structures for Sr_xNbO_3 and Eu_xNbO_3 deduced from the results of the present XPS and UPS studies are given in Figs. 4(a) and 4(b), respectively. In these two energy diagrams, both Sr_xNbO_3 and Eu_xNbO_3 have partially filled bands if no correlations between *d* electrons exist. Shaded area represents the valence-band region. As we previously pointed out,[12] the electric conduction in Sr_xNbO_3 was likely caused by overlaps of the Nb 4*d* and O 2*p* orbitals. This model is

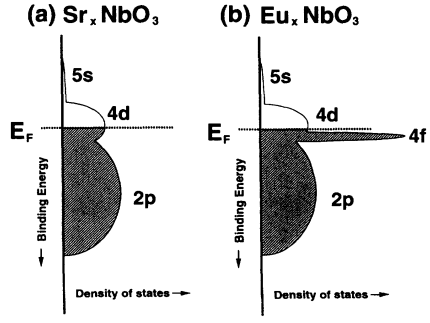

FIG. 4. Schematic electronic structures deduced from the present XPS and UPS studies. Shaded regions correspond to experimentally observed photoemission spectra for (a) Sr_xNbO_3, and (b) Eu_xNbO_3. Note that, the 4*f* levels of Eu_xNbO_3 are not fully filled, but it is not clearly known if the Eu 4*f* states contribute to the conductivity.

essentially the same as Goodenough's model[19] for the tungsten bronze. However, for Eu_xNbO_3, it seems that there are additional contributions from Eu $4f$ to the valence-band region.

With these experimental results of the valence band for Sr_xNbO_3 and Eu_xNbO_3, it is of great interest whether a theoretical band calculation will be available in the near future that supports these results and at the same time correctly predicts the electrical transport properties of these two systems.

IV. CONCLUSION

A photoelectron spectroscopic analysis of the core level and that of valence-band region were studied for Sr_xNbO_3 ($x=0.8$, 0.85, 0.9) and Eu-substituted samples. The valency of the Nb ion was found to be between +4 and +5. From the XPS measurements, core-level spectra, i.e., O $1s$, Sr $3p$, Sr $3d$, and Nb $3d$ spectra, were not changed with varied x. For all samples, sharp Fermi edges were observed only in the case of He I UPS but not for He II UPS or XPS cases. The valence band of Sr_xNbO_3 primarily consisted of the hybridization between the O $2p$ and Nb $4d$ orbitals, as had been proposed for the tungsten bronze by Goodenough. Moreover, a sharp peak of Eu $4f$ state was clearly observed near E_F for Eu-substituted $(Sr, Eu)_{0.9}NbO_3$ samples.

ACKNOWLEDGMENTS

The authors would like to thank Professor S. Tanaka and Professor T. Sakudo of SRL-ISTEC for their continuous support. This work was supported by the New Energy and Industrial Technology Development Organization for the R&D of Industrial Science and Technology Frontier Program.

[1]R. J. Cava, P. Gammel, B. Batlogg, J. J. Krajewski, W. F. Peck, Jr., L. W. Rupp, Jr., R. Felder, and R. B. van Dover, Phys. Rev. B **42**, 4815 (1990).

[2]A. Nozaki, H. Yoshikawa, T. Wada, H. Yamauchi, and S. Tanaka, Phys. Rev. B **43**, 181 (1991).

[3]A. Fujimori, I. Hase, H. Namatame, Y. Fujishima, Y. Tokura, H. Eisaki, S. Uchida, K. Takegahara, and F. M. F. de Groot, Phys. Rev. Lett. **69**, 1796 (1992).

[4]Y. Aiura, F. Iga, Y. Nishihara, H. Ohnuki, and H. Kato, Phys. Rev. B **47**, 6732 (1993).

[5]M. Kasuya, Y. Tokura, T. Arima, H. Eisaki, and S. Uchida, Phys. Rev. B **47**, 6197 (1993).

[6]M. S. Hegde, P. Barboux, C. C. Chang, J. M. Tarascon, T. Venkatesan, X. D. Wu, and A. Inam, Phys. Rev. B **39**, 4752 (1989).

[7]R. Itti, I. Tomeno, K. Ikeda, K. Tai, N. Koshizuka, and S. Tanaka, Phys. Rev. B **43**, 435 (1991).

[8]R. Claessen, M. G. Smith, J. B. Goodenough, and J. W. Allen, Phys. Rev. B **47**, 1788 (1993).

[9]D. Ridgley and R. Ward, J. Am. Chem. Soc. **77**, 6132 (1955).

[10]E. I. Krylov and A. A.Shiarnin, J. Gen. Chem. USSR **25**, 1637 (1955).

[11]B. Hessen, S. A. Sunshine, T. Siegrst, and R. Jimenez, Mater. Res. Bull. **26**, 85 (1991).

[12]K. Isawa, J. Sugiyama, K. Matsuura, A. Nozaki, and H. Yamauchi, Phys. Rev. B **47**, 2849 (1993).

[13]K. Isawa, J. Sugiyama, and H. Yamauchi, Phys. Rev. B **47**, 11 426 (1993).

[14]K. Isawa, R. Itti, J. Sugiyama, N. Koshizuka, and H. Yamauchi, Phys. Rev. B **48**, 7618 (1993).

[15]K. Isawa, J. Sugiyama, and H. Yamauchi, Jpn. J. Appl. Phys. (to be published).

[16]C. D. Wagner, W. M. Riggs, L. E. Davis, J. F. Moulder, and G. E. Muilenberg, *Handbook of X-Ray Photoelectron Spectroscopy* (Perkin-Elmer, Eden Prairie, MN, 1979).

[17]J. J. Yeh and I. Lindau, At. Nucl. Data Tables **32**, 28 (1985).

[18]K. E. Smith and V. E. Henrich, Phys. Rev. B **38**, 9571 (1988).

[19]J. B. Goodenough, in *Progress in Solid State Chemistry,* edited by H. Reiss (Pergamon, Oxford, 1971), Vol. 5, p. 145.

[20]L. F. Mattheiss, Phys. Rev. **181**, 987 (1969).

[21]R. J. Cava, B. Batlogg, J. J. Krajewski, H. F. Poulsen, P. Gammel, W. F. Peck, Jr., and L. W. Rupp, Jr., Phys. Rev. B **44**, 6973 (1991).

[22]T. Tsuda, K. Nasu, A. Yanase, and K. Siratori, *Electronic Conduction in Oxides* (Springer-Verlag, Tokyo, 1991).

[23]B. L. Chamberland and P. S. Danielson, J. Solid State Chem. **3**, 243 (1971).

[24]K. Ishikawa, G. Adachi, M. Hasegawa, K. Sato, and J. Shiokawa, J. Electrochem. Soc. **128**, 1374 (1981).

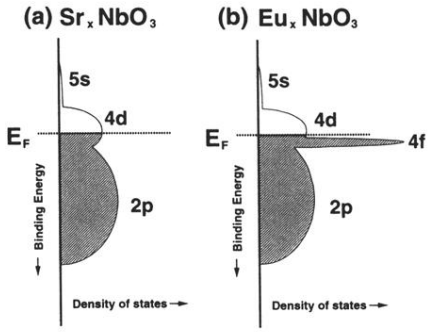

FIG. 4. Schematic electronic structures deduced from the present XPS and UPS studies. Shaded regions correspond to experimentally observed photoemission spectra for (a) Sr_xNbO_3, and (b) Eu_xNbO_3. Note that, the $4f$ levels of Eu_xNbO_3 are not fully filled, but it is not clearly known if the Eu $4f$ states contribute to the conductivity.